International Journal of Heat and Technology
Vol. 43, No. 6, December, 2025, pp. 2313-2322
Journal homepage: http://iieta.org/journals/ijht

Hybrid SPH and Experimental Modeling for Stability Evaluation of a Floating Portable Toilet in Flood-Prone Environments

Muhammad Fauzi[1], Eldina Fatimah[1*], Iqra Mona Meilinda[1], Juellyan Iskandar[2], Muhammad Hafiz Aslami[3]

[1] Department of Civil Engineering, Universitas Syiah Kuala, Banda Aceh 23111, Indonesia
[2] Doctoral Program, School of Engineering, Post Graduate Program, Universitas Syiah Kuala, Banda Aceh 23111, Indonesia
[3] Department of Civil Engineering, Binus University, Jakarta 11480, Indonesia

Corresponding Author Email: eldinafatimah@usk.ac.id

Copyright: ©2025 The authors. This article is published by IIETA and is licensed under the CC BY 4.0 license (http://creativecommons.org/licenses/by/4.0/).

https://doi.org/10.18280/ijht.430629

Received: 1 November 2025
Revised: 19 December 2025
Accepted: 26 December 2025
Available online: 31 December 2025

Keywords:
Smoothed Particle Hydrodynamics (SPH), floating portable toilet (FPT), Response Amplitude Operator (RAO), heave, pitch, surge

ABSTRACT

Floating portable toilets (FPT) are a practical sanitation solution for flood-prone areas, but their dynamic response to waves has not yet been quantitatively validated. This study presents an experimental and numerical validation framework to evaluate the accuracy of the Smoothed Particle Hydrodynamics (SPH) method in predicting the motion response of FPTs to regular waves. Laboratory-scale physical model testing was replicated numerically using SPH with equivalent wave conditions, mooring configurations, and particle resolutions. Surge, heave, and pitch motion responses were analyzed using the Response Amplitude Operator (RAO) and quantified through the percentage of amplitude difference (ΔA%). The results show that the heave mode has the most consistent pattern across the frequency range, although the numerical amplitude tends to be reduced with a relatively smaller negative ΔA% compared to other modes (-72.64% to -39.88%). The pitch response shows greater deviation, with a flatter numerical RAO peak, reflecting sensitivity to the inertia representation and the hydrostatic restoring force. The surge mode shows pattern consistency at low frequencies, but produces the greatest amplitude deviation with ΔA% reaching tens of percent (-92.59% to 35.75%). These findings indicate that SPH accuracy is highly dependent on motion mode characteristics and is influenced by numerical damping parameters, particle resolution, and mooring modeling. This study provides a quantitative basis for applying SPH in the preliminary safety evaluation and design of floating sanitation systems in flood-prone areas and emphasizes the need to calibrate parameters to improve the reliability of field-scale predictions.

1. INTRODUCTION

Flooding is one of the most frequent hydrometeorological disasters in various regions of Indonesia, particularly in areas with high rainfall intensity, lowland topography, or inadequate drainage systems [1, 2]. The impacts of flooding extend beyond material losses, infrastructure damage, and disruption of community activities; they also pose significant public health risks due to deteriorating sanitation conditions.

In emergency flood situations, conventional sanitation systems such as permanent toilets become unusable due to inundation, structural damage, or loss of access [3]. This increases the risk of waterborne diseases such as diarrhea, leptospirosis, and skin infections [4-6]. Therefore, emergency sanitation solutions capable of operating effectively in flood-affected areas are urgently needed, one of which is the use of floating portable toilets (FPTs).

The concept of an FPT combines portability with buoyancy, enabling its use even when land-based infrastructure is non-functional. While this idea offers a practical solution, its primary challenge lies in ensuring structural stability under dynamic flood currents and wave conditions. Instability may compromise user comfort, increase the risk of capsizing, and pose safety hazards. Thus, stability assessment becomes a critical aspect prior to field implementation [7, 8].

Previous studies on floating structures have primarily focused on boats, pontoons, or floating platforms, emphasizing hydrostatic analysis and hydrodynamic behavior rather than sanitation-specific applications such as floating toilets. Research on hydrostatic stability of pontoons and floating structures often employs classical hydrostatic analysis and GZ curve evaluation for initial stability assessment [9].

Additionally, experimental and numerical investigations into dynamic motion and hydrodynamic responses of pontoons under wave, wake, and current conditions are essential for determining hydro-elastic coupling in floating structures [10]. Alternatively, particle-based or mesh-free methods such as Smoothed Particle Hydrodynamics (SPH) have gained attention for their ability to simulate highly nonlinear free-surface flows, breaking waves, and strong fluid structure interactions (FSIs). SPH has been validated through numerical and experimental studies for semi-submersible and pontoon applications [11].

Important studies have also been conducted in Japan on operational safety and comfort limits [12]. On the numerical side, grid-based Computational Fluid Dynamics (CFD) and

FSI methods are widely used to model FSIs in floaters and offshore platforms, particularly in the context of floating offshore wind turbines (FOWTs). Recent reviews highlight the critical role of CFD/FSI in addressing flow complexity, nonlinear wave behavior, and highlighting sanitation challenges in post-disaster evacuation centers, where damage to basic infrastructure, such as water supply, drainage, and waste treatment, hinders survival and recovery.

One innovation developed is a mobile flush toilet that provides sanitation services equivalent to permanent toilets without relying on existing infrastructure. This technology has been deployed in three flood response operations in Japan and installed on islands and public areas as a sustainable solution to daily sanitation challenges. The implementation of mobile flush toilets has proven effective in enhancing disaster-resilient infrastructure while preserving user dignity, health, and safety in emergencies [13].

A highly relevant study in Indonesia focused on estimating clean water requirements and wastewater treatment systems for FTP in flood-prone areas. The study employed qualitative analysis of water and waste systems along with analytical calculations to determine water demand. It demonstrated that FTP could serve as an environmentally friendly sanitation solution in inundated regions, while also promoting sustainable technology development. Although the study shares the same object of interest, its focus was on water and waste system design rather than structural stability under flood conditions [8].

The novelty of the present study lies in the integration of numerical SPH methods with laboratory-scale experimental testing to evaluate the stability of FTP under flood conditions. The SPH method, as implemented in the DualSPHysics software, enables simulation of free-surface fluid phenomena with complex geometries and strong fluid–structure interactions [14]. Unlike grid-based CFD, which faces limitations in modeling extreme free-surface deformations, SPH is mesh-free and capable of realistically representing irregular waves and multiphase interactions [15].

This approach offers advantages over previous methods that relied solely on hydrostatic analysis or single-mode numerical simulations. By combining SPH simulation with experimental testing, direct validation can be achieved, resulting in more reliable outcomes.

Furthermore, testing under flood conditions with varying wave heights, wave periods, and current velocities will generate a comprehensive dataset for developing safer and more user-friendly designs. The objective of this study is to verify and compare simulation results through physical testing in a hydraulic laboratory against numerical modeling outcomes. The findings will likely contribute to the development of effective, safe, and widely applicable emergency sanitation solutions for disaster-affected regions.

2. MATERIAL AND METHODS

2.1 Floods

Flooding is a hydrometeorological phenomenon that causes significant physical, economic, and human losses [16]. Flooding is the most frequent natural disaster worldwide and has caused severe damage [17]. In Indonesia, floods have consistently ranked among the most common disasters between 2012 and 2022, placing second in frequency according to data released by the National Disaster Management Agency [18]. Floods are primarily triggered by high rainfall and densely populated settlements along riverbanks [19]. Due to their topographic characteristics, low-lying areas are particularly vulnerable to flooding [20]. Flood risk arises from climate change and the lack of public awareness and environmental responsibility [21]. The impact of flooding has expanded significantly across various regions of the world, especially in tropical countries. Climate change driven by global warming is often cited as a key factor behind rainfall's increasing intensity and duration, directly contributing to broader flood exposure [22].

2.2 Waves

Ocean waves are complex dynamic phenomena [23] triggered by wind forces, submarine earthquakes, volcanic eruptions, and tectonic movements [24, 25]. Their characteristics include wave height, wavelength, period, and propagation speed. Waves are periodic water motions influenced primarily by wind, with substantial implications for marine navigation and coastal infrastructure [26]. They may form under extreme weather conditions or seismic events, affecting shoreline morphology and maritime activities.

2.3 Floating portable toilet

2.3.1 Toilet

According to the Indonesian Ministry of Public Works and Housing [27], a toilet is a designated sanitary facility equipped with a water closet, clean water supply, and other hygienic components, designed to meet physical, social, and psychological needs in domestic, commercial, and public settings. Toilets serve as sanitation infrastructure for defecation, urination, and personal hygiene [28]. Public toilets are inclusive facilities accessible to all individuals regardless of age or gender.

2.3.2 Portable toilet

According to the Indonesian Standard Book for Public Toilets [29] issued by the Ministry of Culture and Tourism, public toilets are sanitation facilities intended for general use without demographic restrictions. The term "portable" refers to the ease of transport and relocation. In sanitation, a portable toilet is a movable unit that can be installed and dismantled.

2.3.3 Floating portable toilet

A toilet is a device or facility designed for human excretory functions. According to linguistic definitions and expert interpretations, "portable" denotes ease of transport, while "floating" refers to buoyancy or the ability to remain on the water's surface. Thus, an FTP is a modular sanitation unit easily assembled, disassembled, and deployed on water bodies.

The FTP represents an innovative sanitation solution engineered for mobility, rapid installation, and aquatic stability [30]. Its primary advantage lies in its practicality and adaptability to submerged or flood-prone areas. The selection of design criteria and construction materials prioritizes structural stability and operational effectiveness in floating conditions.

2.4 Portable toilet (FPT) model

Numerical modeling was previously conducted in a study by Munir et al. [31]. The numerical model used is shown in Figure 1(a) and represents a simplified version of the earlier model developed by Diyatura [32]. For the physical modeling, a scaled-down model was constructed with a geometric scale ratio of 1:10, resulting in a physical model smaller than its numerical counterpart (Figure 1(b)). During testing, the applied loads corresponded to the maximum and minimum load conditions that the test model could accommodate.

The Froude similarity principle was employed as the basis for determining model similarity. The geometric scale is defined as NL = Lp/Lm. Based on Froude similarity, additional scaling parameters, namely time and weight, were derived. These scaling relationships can be expressed as a length scale and a weight scale, NL = 10 and weight scale $NL^3 = 10^3 = 1000$. The corresponding model dimensions and other parameters are presented in Table 1.

Table 1. Dimensional comparison between the numerical and physical design of the FPT model at a 1:10 scale

Model Component	Numerical Model Dimensions	Experimental Model Dimensions
Floor	5.2 m × 2.6 m × 1.0 m	52 cm × 26 cm × 10 cm
Wall	3.2 m × 1.6 m × 2.2 m	32 cm × 16 cm × 22 cm
Water Tank (Torent)	0.6 m × 0.9 m	6 cm × 9 cm
Water Drum	0.6 m × 2.0 m	6 cm × 20 cm
Floating Concrete Block	3.6 m × 1.0 m × 0.8 m	36 cm × 10 cm × 8 cm
Draft (S)	0.6 m	6 cm
Minimum Weight (Wmin)	2798 kg	2.8 kg
Maximum Weight (Wmax)	4131 kg	4.1 kg

The wave variations used in both numerical and physical model testing were also scaled at a ratio of 1:10. The wave parameters applied in both tests are presented in Table 2. The selected wave heights reflect operational conditions in which the floating structure is intended to be deployed. Estuarine environments such as the Krueng Aceh River may experience dynamic conditions and significant wave activity due to external marine influences and human activities. The FPT is designed for use in waters with wave heights up to 1.5 meters; therefore, wave variations of 5 cm, 10 cm, and 15 cm in the physical model are considered appropriate representations.

Table 2. Wave height variations used in numerical and physical model testing

Parameter	Numerical Model Variation (m)	Experimental Model Variation (cm)	Description
Wave Height (*H*)	0.50	5	Small wave
	1.00	10	High wave
	1.50	15	Extreme wave

2.5 Methods

2.5.1 Numerical modelling

The numerical modeling employed the SPH method, a mesh-free approach in CFD. The SPH simulation was conducted in three dimensions, focusing on floating behavior, with an inter-particle spacing of 0.12 m and a total of 396,792 particles. The simulation was performed using the DualSPHysics software.

This particle-based CFD method assigns properties such as velocity, position, and direction to each simulated object. SPH utilizes interpolation techniques to compute physical quantities at a given point or particle, where each particle's properties are calculated based on neighboring particles within a defined smoothing length. Wave height served as the key parameter for comparison in the numerical simulation. Wave elevation was measured using two wave probes positioned 1 meter upstream and downstream of the FTP.

The SPH method was chosen because it offers significant advantages for the study of free flow and fluid-structure interactions, which are difficult to handle with traditional mesh-based CFD methods. A critical question in the field is how to effectively model these complex interactions without resorting to cumbersome mesh adjustments and remeshing processes, which often lead to inaccuracies and increased computational costs.

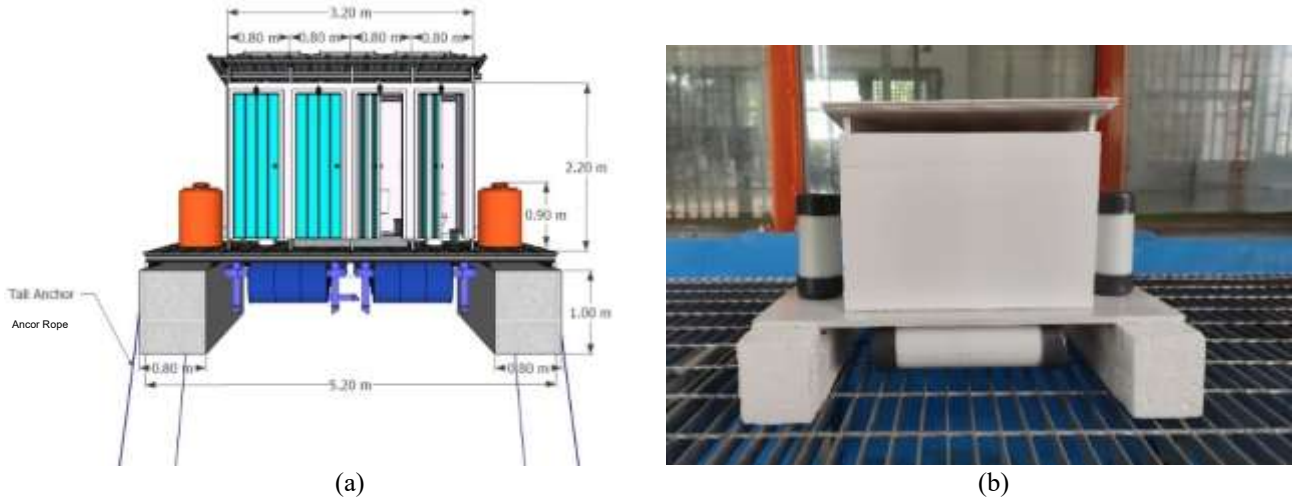

(a) (b)

Figure 1. Design model floating toilet portable, (a) numerical model, (b) experimental model

SPH addresses this challenge with its mesh-free Lagrangian approach, as it does not require a fixed mesh, thus allowing large geometric deformations, free-surface formation, and interactions with moving structures to be naturally formulated without the complex remeshing often required in Eulerian methods. This particle approach directly tracks the fluid's position, facilitating the handling of complex interfaces and phases while ensuring advection continuity without interface reconstruction, as in VOF or Level-Set.

The mesh-free character and Lagrangian nature of SPH also enhance robustness against free-surface and multiphase flows, as well as dynamic impacts, which are relevant to high-wave studies and interactions with floating structures, as discussed in this research. In summary, SPH provides greater flexibility and accuracy in modeling flows with large deformations and free-surface dynamics compared to conventional grid-based CFD methods, albeit at a higher computational cost that is now increasingly manageable through modern parallelization techniques [33, 34].

2.5.2 Experimental modelling

The physical stability testing of the FTP model was conducted using a flume facility located at the Tsunami and Disaster Mitigation Research Center (TDMRC), Universitas Syiah Kuala. The flume is capable of simulating specific tsunami wave models. Additionally, the apparatus can generate regular and irregular waves, wind-induced waves, and current-driven flow variations (discharge variations).

2.5.3 Testing scenarios

The testing scenarios, which include variations in load conditions and wave types, are presented in Table 3. They are designed to ensure that the model performs as expected under a range of possible conditions.

Table 3. Testing scenarios

Test Type	Load Scenario	Wave Condition	Notation
H1 (Horizontal)	Empty Condition (Minimum Weight, *W*min)	Small wave	HKG1
		High wave	HKG2
		Extreme wave	HKG3
	Full Condition (Maximum Weight, *W*max)	Small wave	HPG1
		High wave	HPG2
		Extreme wave	HPG3
V2 (Vertical)	Empty Condition (Minimum Weight, *W*min)	Small wave	VKG1
		High wave	VKG2
		Extreme wave	VKG3
	Full Condition (Maximum Weight, *W*max)	Small wave	VPG1
		High wave	VPG2
		Extreme wave	VPG3

3. RESULT AND DISCUSSION

3.1 Physical model testing

Prior to conducting the physical model tests, several preparations were required. To generate waves within the flume, appropriate amplitude and frequency configurations were needed for the wave generator setup. Preliminary trials were conducted to determine the configuration that matched the target wave conditions for testing. The final wave configuration obtained from instrument calibration is presented in Table 4.

Table 4. Instrument test results for wave generator settings

Target Wave Height (cm)	Flume Settings	
	Frequency (Hz)	Amplitude (cm)
5	0.40	0.03
10	0.40	0.06
15	0.22	0.10

The next stage involved the installation of the model and loading system. During the installation process, the model nearly capsized several times due to stiffness in the connecting rope. At this stage, testing of the effective rope length was carried out. The first trial used a connecting rope with a length of 90 cm (Figure 2(a)). Under 5 cm wave conditions, the rope stiffness remained within a normal and safe range. However, when tested under 10 cm wave conditions, the rope became rigid and caused the model to overturn. A second trial was conducted using a 110 cm connecting rope (Figure 2(b)). The results of the second trial showed that the 110 cm rope was effective in maintaining model stability without significant stiffness, thereby allowing unobstructed movement of the model during analysis.

3.2 Model stability simulation

Model stability simulations were conducted using four scenarios: HKG, HPG, VKG, and VPG, as described in Table 3. The simulation results provided values for surge (translational movement), pitch (rotational movement), and heave (vertical movement) under two wave directions: horizontal (HKG and HPG) and vertical (VKG and VPG). The simulation outcomes for both directions are presented in Table 5. Based on the comparative results, both numerical and experimental tests consistently indicate that the portable floating toilet remains stable and safe, even when subjected to wave conditions ranging from mild to extreme, under both minimum and maximum loading scenarios.

3.3 Response Amplitude Operator (RAO)

The RAO analysis was conducted to normalize the data, enabling a clearer comparison of the dynamic behavior between the two sets of results. The RAO analysis results are tabulated in Table 6. These results are further illustrated as comparative curves shown in Figure 3. Figure 3 presents the RAO curve comparisons for heave (Figure 3(a)), pitch (Figure 3(b)), and surge (Figure 3(c)) between experimental testing and numerical simulation based on SPH.

In the heave mode, the quantitative discrepancy indicates a tendency for underprediction in the SPH model, where the numerically computed vertical response is lower than the actual response measured in the laboratory. This condition may be attributed to several factors, including relatively high numerical damping due to artificial viscosity settings, insufficient particle resolution to capture fluid–structure interactions accurately, or minor differences in boundary representation and model geometry between the simulation and physical testing.

(a)

(b)

Figure 2. Testing of effective connecting rope length for the model: (a) rope length 90 cm, (b) rope length 110 cm

Table 5. Comparison of numerical and experimental simulation results

Trial	DOF							
	Experimental				Numerical			
	Heave	Pitch	Surge	Stability Pitch < 15°	Heave	Pitch	Surge	Stability Pitch < 15°
HKG1	0.44	3.15	1.35	Safe	0.20	4.00	0.10	Safe
HKG2	0.88	4.91	1.67	Safe	0.30	6.00	0.20	Safe
HKG3	1.46	13.31	1.01	Safe	0.40	6.00	0.30	Safe
HPG1	0.45	3.08	0.57	Safe	0.20	3.00	0.10	Safe
HPG2	0.90	6.59	2.43	Safe	0.30	5.00	0.20	Safe
HPG3	1.43	16.56	2.62	Safe	0.40	5.00	0.30	Safe
VKG1	0.50	1.93	0.22	Safe	0.30	3.00	0.30	Safe
VKG2	0.82	5.38	0.73	Safe	0.50	6.00	0.50	Safe
VKG3	1.78	8.99	2.87	Safe	0.50	6.00	0.60	Safe
VPG1	0.47	1.76	0.85	Safe	0.20	2.00	0.20	Safe
VPG2	0.82	6.38	1.47	Safe	0.40	5.00	0.30	Safe
VPG3	1.75	9.17	1.88	Safe	0.50	6.00	0.40	Safe

Table 6. Analysis of the RAO

Trial	RAO					
	Experimental			Numerical		
	Heave	Pitch	Surge	Heave	Pitch	Surge
HKG1	0.88	6.30	2.70	0.40	8.00	0.20
HKG2	0.88	4.91	1.67	0.30	6.00	0.20
HKG3	0.97	8.87	0.67	0.27	4.00	0.20
HPG1	0.89	6.16	1.14	0.40	6.00	0.20
HPG2	0.90	6.59	2.43	0.30	5.00	0.20
HPG3	0.95	11.04	1.75	0.27	3.33	0.20
VKG1	1.00	3.86	0.44	0.60	6.00	0.60
VKG2	0.82	5.38	0.73	0.50	6.00	0.50
VKG3	1.19	5.99	1.91	0.33	4.00	0.40
VPG1	0.93	3.52	1.69	0.40	4.00	0.40
VPG2	0.82	6.38	1.47	0.40	5.00	0.30
VPG3	1.17	6.11	1.25	0.33	4.00	0.27

Nevertheless, the numerical curve still exhibits a response amplification pattern at mid-range frequencies that resembles the experimental trend. This suggests that the SPH model has captured part of the dynamic characteristics of the structure under wave loading. Similar findings have been reported in studies involving SPH modeling of floating structures such as FOWTs, where validation against experimental data showed good consistency—but only after careful calibration of parameters such as mooring and numerical viscosity [35].

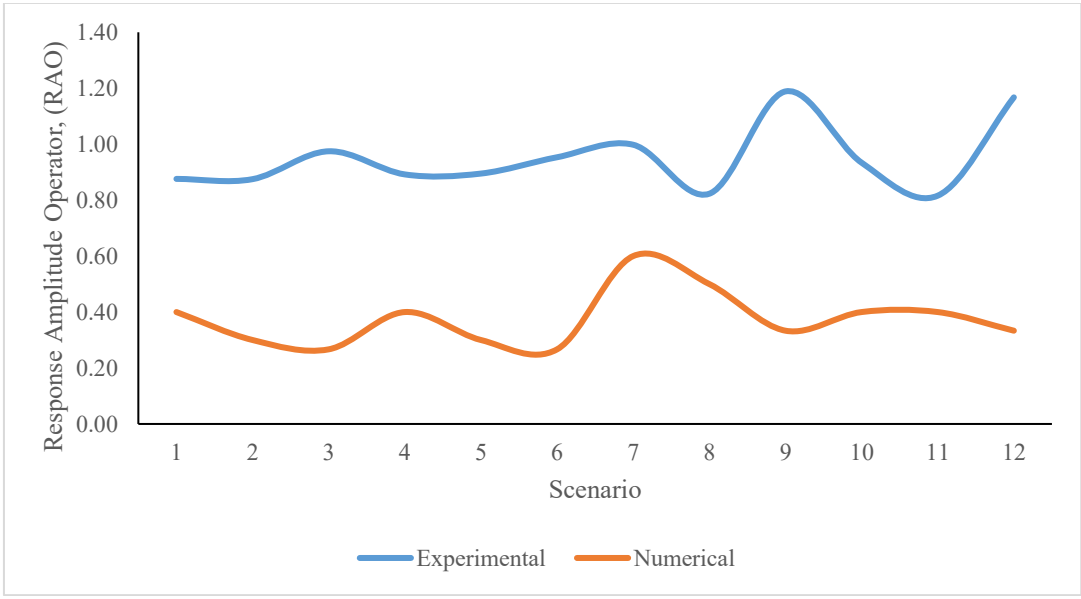

(a)

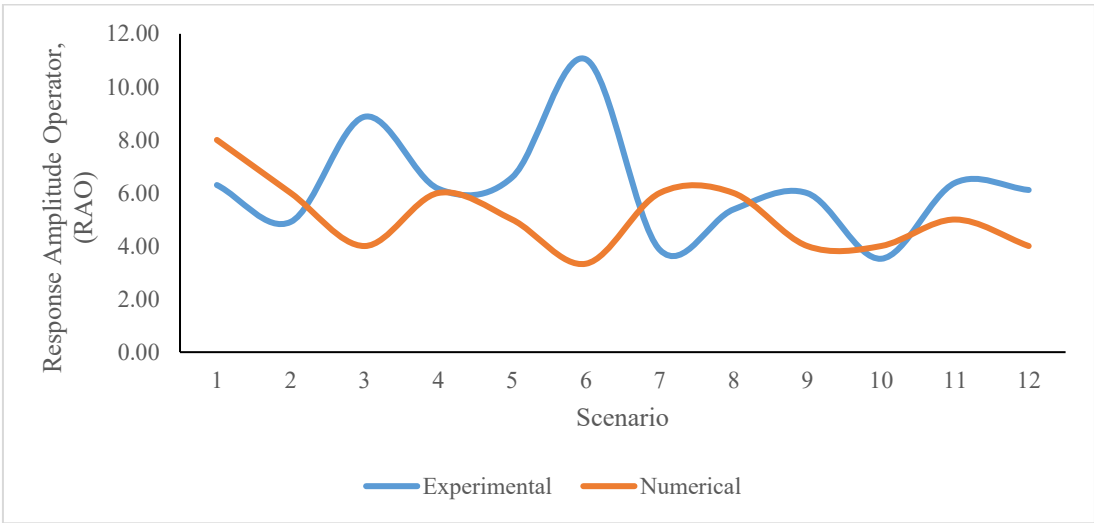

(b)

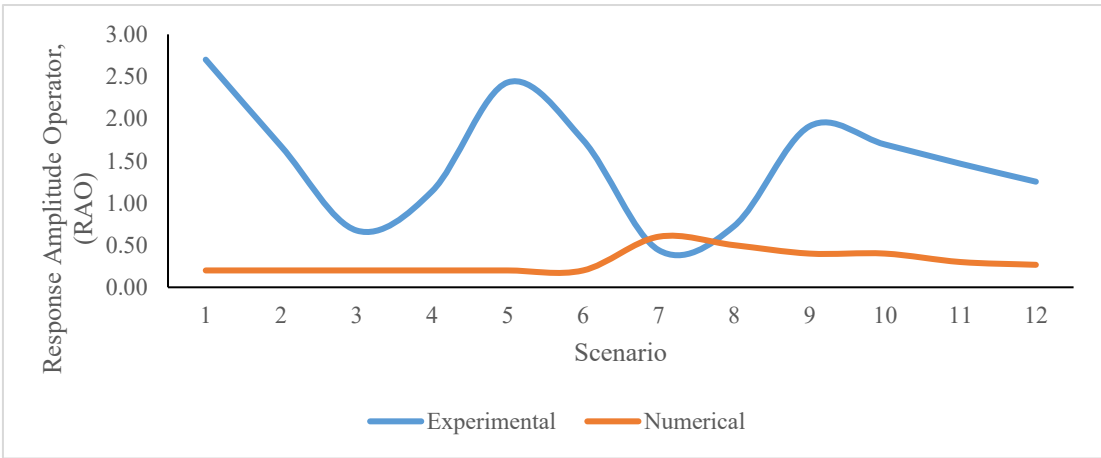

(c)

Figure 3. RAO analysis, (a) heave, (b) pitch, and (c) surge

In the pitch response, a relative discrepancy is also observed, with the experimental RAO exhibiting a sharp peak, while the numerical simulation produces a broader and more flattened curve. This likely reflects the sensitivity to moment of inertia and the influence of hydrostatic restoring forces, which the numerical model may not fully capture. A parametric approach combined with mooring coefficient tuning has proven effective in reproducing pitch RAO trends in spar-type floating structures, where such calibration helps compensate for inaccuracies in inertia estimation and flow assumptions within potential theory [36, 37].

Unlike the other two modes, the surge response shows the largest amplitude deviation between experimental and numerical results, particularly at mid to high frequencies. Nevertheless, the fluctuation pattern at low frequencies still exhibits a similar shape, indicating that the SPH model has limitations in accurately representing horizontal translational dynamics across the full frequency range. This significant discrepancy may be attributed to the surge mode's sensitivity to boundary conditions, viscous drag representation, and more complex wave–body interactions in the lateral direction [38, 39].

Overall, the consistent quantitative differences, especially the tendency for amplitude underprediction, are likely caused by SPH parameter settings such as artificial viscosity, particle spatial resolution, and suboptimal boundary condition representation. However, the similarity in RAO curve trends suggests that the core model adequately captures the structure's dynamic characteristics. As illustrated in the aforementioned FOWT study, a more accurate representation of mooring dynamics and surrogate parameters such as moment of inertia is crucial for reducing numerical discrepancies in RAO predictions [35].

Therefore, further calibration efforts on the SPH model are strongly recommended, including adjustments to numerical viscosity, enhancement of particle resolution, and refinement of boundary conditions, to achieve better quantitative agreement with experimental data. With sufficient validation and calibration, the SPH model holds significant potential as a reliable predictive tool for studying equilibrium and dynamic responses of floating structures even under more complex wave conditions and supports practical applications in advanced marine engineering.

3.4 Percentage difference in amplitude (ΔA%)

The amplitude difference (ΔA%) was calculated to quantify the relative error between numerical simulation and experimental results. The computed values are presented in Table 7. The comparison results indicate that ΔA% for heave is predominantly negative across all test scenarios, suggesting that the numerical response (SPH) tends to underpredict the experimental data. This pattern is consistent with previous SPH validation studies for floating structures, where artificial viscosity often contributes to increased effective damping, resulting in lower computed vertical motion amplitudes compared to physical measurements unless dissipation parameters and particle resolution are carefully calibrated. Recent literature highlights that dissipation scheme settings in SPH directly affect wave energy attenuation and response peaks, making RAO curves and derived metrics such as ΔA% highly sensitive to these parameter choices [39].

For pitch, ΔA% exhibits wider variation, with instances of overprediction (positive ΔA%) at lower amplitudes, shifting toward underprediction at higher amplitudes. This behavior is common when the effective moment of inertia, hydrostatic restoring stiffness, and wave structure coupling are not fully represented in the numerical model. Comparative studies on modern floating structures report that reproducing sharp RAO pitch peaks near resonance frequencies typically requires calibration of stiffness and mooring components, or hybrid modeling approaches to prevent numerical amplitude flattening. This trend aligns with the observed ΔA% sign shifts across excitation levels, indicating high sensitivity of rotational modes to model parameters [40, 41].

Table 7. Percentage difference in amplitude (ΔA%)

Trial	Amplitude Wave	ΔA%		
		Heave	Pitch	Surge
HKG1	0.50	-54.34	26.98	-92.59
HKG2	1.00	-65.71	22.20	-88.04
HKG3	1.50	-72.64	-54.92	-70.30
HPG1	0.50	-55.16	-2.60	-82.46
HPG2	1.00	-66.48	-24.13	-91.77
HPG3	1.50	-72.03	-69.81	-88.55
VKG1	0.50	-39.88	55.44	35.75
VKG2	1.00	-39.25	11.52	-31.03
VKG3	1.50	-71.96	-33.26	-79.06
VPG1	0.50	-57.17	13.64	-76.39
VPG2	1.00	-50.98	-21.63	-79.54
VPG3	1.50	-71.44	-34.57	-78.71

Unlike the heave mode, which shows the most consistent pattern, surge yields the largest ΔA% values across most frequency ranges, indicating significant amplitude discrepancies relative to experimental results. Nevertheless, at low frequencies, the surge still displays a replicable trend in SPH simulations, consistent with the nature of longitudinal translation being more directly influenced by linear wave forces.

These quantitative differences are likely affected by damping representation and boundary condition settings in the numerical model. Several experimental–numerical studies on floating platforms have found that surge and heave responses can achieve good agreement after tuning damping and mooring characteristics, which is reflected in a systematic reduction of ΔA% values relative to experimental data [38, 39].

Methodologically, ΔA% calculations should be performed for both test types. According to ITTC documentation [23], quantifying test uncertainty and ensuring transparent numerical–experimental validation practices, including reporting relative errors or percent differences per test condition, is essential. Based on these guidelines, small and consistent ΔA% values across conditions are more meaningful than coincidental matches at isolated points; conversely, large and systematic ΔA% values (e.g., consistently negative across all levels) indicate model bias that should be addressed through calibration of dissipation parameters, particle resolution, and boundary condition alignment [42].

The practical implications of ΔA% observations are as follows: the dominance of negative ΔA% in heave and surge suggests a conservative bias, where the numerical model tends to underestimate responses. While this may be acceptable for preliminary studies, it risks obscuring peak loads in limit-state design applications.

Meanwhile, the variability of ΔA% in pitch underscores the need for multi-level calibration: (i) adjusting numerical viscosity and particle spacing to reduce over-damping, (ii)

refining mooring representation and inertia properties to preserve RAO peak sharpness, and (iii) re-verifying wave condition equivalence between test facilities and numerical domains. Previous studies on wave energy devices and floating wind platforms have shown that after implementing these steps, amplitude agreement assessed via RAO and derived metrics improves significantly relative to experimental data [35, 43].

To put the relative amplitude differences (ΔA%) obtained in this study into context, it is important to consider typical error levels reported in the literature on motion response predictions. Experimental uncertainty analyses in seakeeping tests have demonstrated that, under controlled laboratory conditions, expanded uncertainty in RAO measurements for heave and pitch motions can be quite small: heave RAO measurements often exhibit uncertainties below 3% and pitch RAO uncertainties below 1% at a 95% confidence level when standardized procedures are applied.

These narrow uncertainty bounds reflect the precision achievable in high-quality experimental facilities and provide a benchmark for understanding the measurement error inherent in physical tests [44].

Comparatively, the ΔA% values obtained in the present work span a wider range: for heave, ΔA% varies between 72.64% and -39.25%; for pitch, ΔA% ranges from -69.81% to 55.44%; and for surge, ΔA% ranges from -92.59% to 35.75%.

The magnitudes of these differences exceed typical experimental measurement uncertainty and are comparable to, or larger than, motion prediction errors reported in comprehensive validation studies for seakeeping and motion response modelling, where average errors in motion amplitudes relative to experimental data have been reported on the order of tens of percent across different methods and conditions.

This comparison highlights a common characteristic of numerical predictions of motion in complex fluid–structure interaction problems: while numerical methods can capture overall trends in motion response, quantitative discrepancies with experimental results often arise from limitations in modelling damping, viscous effects, and boundary conditions. Within this context, the ΔA% values for heave and pitch indicate areas where the current SPH model may benefit from further refinement, whereas the relatively narrower ΔA% observed in some surge conditions suggests that longitudinal motion predictions may be less sensitive to certain aspects of model configuration under specific test conditions. Collectively, these comparisons provide a meaningful assessment of the current model's performance and clearly identify specific motion modes for targeted improvement in future work.

3.5 Applicable scope of the model

The applicability of the proposed SPH model is currently confined to the range of working conditions investigated in this study. The model has been validated under regular wave excitation at laboratory scale, with fixed geometric configuration and mooring arrangement. Within this scope, the SPH model demonstrates consistent capability to reproduce the heave response of the FTP, as indicated by the similarity in RAO trends across the tested frequency range.

For the pitch motion, the model captures the general response pattern; however, noticeable amplitude discrepancies are observed at certain frequencies, suggesting sensitivity to rotational dynamics and to the damping representation. The surge response shows the largest deviation from experimental results, particularly at medium to high frequencies, suggesting that the current SPH configuration is less reliable for accurately predicting longitudinal motion under these conditions.

Accordingly, the current model is most applicable for preliminary stability and motion assessments of FTP subjected to regular waves with small to moderate amplitudes. Its application to irregular wave conditions, extreme wave environments, or full-scale scenarios should be approached with caution, as these conditions have not been explicitly validated in the present study. Further model refinement and additional validation are required before extending the model to broader operational conditions.

4. CONCLUSIONS

The comparative analysis between experimental data and numerical simulations based on SPH reveals that the model's ability to reproduce motion response patterns of floating structures varies significantly across modes. The heave mode demonstrates the most consistent pattern similarity across the frequency range, although amplitude discrepancies are evident.

The pitch mode exhibits greater deviations in both pattern and amplitude, likely influenced by the complexity of wave structure interactions associated with the geometry. Meanwhile, the surge mode retains pattern fidelity at low frequencies but yields the highest ΔA% values across most frequency ranges, indicating more pronounced quantitative discrepancies compared to other modes.

The limitations of this study include simplified damping representation, constrained particle resolution in SPH affecting FSI details, and mooring configurations that do not fully reflect field conditions. Furthermore, the wave conditions tested were limited to specific characteristics, necessitating caution in generalizing the findings.

For future research, it is recommended to conduct simulations with varied damping parameters, enhanced mooring configurations, and higher particle resolution to improve predictive accuracy. Incorporating more diverse wave conditions, including random and multi-directional waves, and validating the model under full-scale scenarios may further strengthen its reliability for real-world applications.

ACKNOWLEDGMENT

The authors are grateful for the support of the Institute for Research and Community Service of Syiah Kuala University and the Ministry of Higher Education, Science, and Technology for funding this study through the BIMA contract No. 094/E5/PG.02.00.PL/2024 dated June 11, 2024, and the Syiah Kuala University (USK) contract No. 633/UN11.2.1/PG.01.03/SPK/DRTPM/2024 dated June 12, 2024. The authors also extend their sincere gratitude to the Syiah Kuala University Tsunami and Disaster Mitigation Research Center (TDMRC) laboratory staff and all parties who actively supported the successful completion of this study.

REFERENCES

[1] Yamamoto, K., Sayama, T., Apip. (2021). Impact of climate change on flood inundation in a tropical river basin in Indonesia. Progress in Earth and Planetary Science, 8(1): 5. https://doi.org/10.1186/s40645-020-00386-4

[2] Yanfatriani, E., Marzuki, M., Vonnisa, M., Razi, P., Hapsoro, C.A., Ramadhan, R., Yusnaini, H. (2024). Extreme rainfall trends and hydrometeorological disasters in tropical regions: Implications for climate resilience. Emerging Science Journal, 8(5): 1860-1874. https://doi.org/10.28991/ESJ-2024-08-05-012

[3] Borges Pedro, J.P., Oliveira, C.A.d.S., de Lima, S.C.R.B., von Sperling, M. (2020). A review of sanitation technologies for flood-prone areas. Journal of Water, Sanitation and Hygiene for Development, 10(3): 397-412. http://doi.org/10.2166/washdev.2020.019

[4] van der Heijden, S., Cassivi, A., Mayer, A., Sandholz, S. (2022). Water supply emergency preparedness and response in health care facilities: A systematic review on international evidence. Frontiers in Public Health, 10. https://doi.org/10.3389/fpubh.2022.1035212

[5] Philippe, S., Hueso, A., Kafuria, G., Sow, J., Kambou, H.B., Akosu, W., Beensi, L. (2022). Challenges facing sanitation workers in Africa: A four-country study. Water, 14(22): 3733. https://doi.org/10.3390/w14223733

[6] Berihun, G., Adane, M., Walle, Z., Abebe, M., Alemnew, Y., Natnael, T., Andualem, A., Ademe, S., Tegegne, B., Teshome, D., Berhanu, L. (2022). Access to and challenges in water, sanitation, and hygiene in healthcare facilities during the early phase of the COVID-19 pandemic in Ethiopia: A mixed-methods evaluation. PLOS ONE, 17(5): e0268272. https://doi.org/10.1371/journal.pone.0268272

[7] Strey, B., Aita, J.S.B., Frata, B., Cechetti, F., Pinto, R.S. (2025). Aquatic and land-based therapies were ineffective in improving muscle strength and morphological parameters in Parkinson: A randomized trial. Clinical Biomechanics, 127: 106594. https://doi.org/10.1016/j.clinbiomech.2025.106594

[8] Clara, B.F., Fauzi, M., Fatimah, E., Fauzia, A. (2025). Eco-friendly sanitation system design for floating portable toilets in flood-prone regions. IOP Conference Series: Earth and Environmental Science, 1510(1): 012069. http://doi.org/10.1088/1755-1315/1510/1/012069

[9] Scicluna, D., De Marco Muscat-Fenech, C., Sant, T., Vernengo, G., Tezdogan, T. (2022). Preliminary analysis on the hydrostatic stability of a self-aligning floating offshore wind turbine. Journal of Marine Science and Engineering, 10(12): 2017. https://doi.org/10.3390/jmse10122017

[10] Haider, R., Li, X., Shi, W., Lin, Z., Xiao, Q., Zhao, H. (2024). Review of computational fluid dynamics in the design of floating offshore wind turbines. Energies, 17(17): 4269. https://doi.org/10.3390/en17174269

[11] Tagliafierro, B., Karimirad, M., Altomare, C., Göteman, M., Martínez-Estévez, I., Capasso, S., Domínguez, J.M., Viccione, G., Gómez-Gesteira, M., Crespo, A.J.C. (2023). Numerical validations and investigation of a semi-submersible floating offshore wind turbine platform interacting with ocean waves using an SPH framework. Applied Ocean Research, 141: 103757. https://doi.org/10.1016/j.apor.2023.103757

[12] Freeman, E.L., Splinter, K.D., Cox, R.J., Flocard, F. (2022). Dynamic motions of piled floating pontoons due to boat wake and their impact on postural stability and safety. Journal of Marine Science and Engineering, 10(11): 1633. https://doi.org/10.3390/jmse10111633

[13] Soshino, Y., Miyata, A. (2024). Innovative sanitation system for disaster victims and aocial aanitation challenges. In Disaster Risk Reduction, pp. 159-177. https://doi.org/10.1007/978-981-97-2049-1_9

[14] Altomare, C., Domínguez, J.M., Fourtakas, G. (2022). Latest developments and application of SPH using DualSPHysics. Computational Particle Mechanics, 9(5): 863–866. https://doi.org/10.1007/s40571-022-00499-1

[15] Luo, M., Su, X., Kazemi, E., Jin, X., Khayyer, A. (2025). Review of smoothed particle hydrodynamics modeling of fluid flows in porous media with a focus on hydraulic, coastal, and ocean engineering applications. Physics of Fluids, 37(2): 021303. https://doi.org/10.1063/5.0252125

[16] Abegaz, R., Wang, F., Xu, J. (2024). History, causes, and trend of floods in the US: A review. Natural Hazards, 120(15): 13715-13755. http://doi.org/10.1007/s11069-024-06791-y

[17] Kuswardhana, A.T., Wahyono, R.U.A. (2023). Pemetaan Geospasial Risiko Banjir di Sub-DAS Gunting, Jombang Jawa Timur. Rekayasa Sipil, 17(1): 54-65. https://doi.org/10.21776/ub.rekayasasipil.2023.017.01.8

[18] Rijal, S., Nursaputra, M., Dari, H.U. (2024). Flood susceptibility analysis using frequency ratio method in Walanae watershed. International Journal of Sustainable Development & Planning, 19(3): 823-832. https://doi.org/10.18280/ijsdp.190302

[19] Supani, A., Andriani, Y. (2020). Designing and applying flood early warning system based on waterfall and water level for special of Palembang City. Journal of Physics: Conference Series, 1500(1): 012129. http://doi.org/10.1088/1742-6596/1500/1/012129

[20] Setianto, H., Utaya, S., Bachri, S., Utomo, D.H., Taryana, D. (2025). Urban flood risk management: A study of adaptation based on knowledge of ethnic communities on the banks of the Musi river in Palembang. International Journal of Sustainable Development & Planning, 20(3): 1253-1263. http://doi.org/10.18280/ijsdp.200330

[21] Hosseinzadehtalaei, P., Tabari, H., Willems, P. (2020). Climate change impact on short-duration extreme precipitation and intensity–duration–frequency curves over Europe. Journal of Hydrology, 590: 125249. https://doi.org/10.1016/j.jhydrol.2020.125249

[22] Ishikawa, T., Akoh, R., Senoo, H. (2023). Flood disaster mitigation strategy in the early modern age in Japan (The Beginning of 17th to the Mid-19th Century). International Journal of Environmental Impacts, 6(1): 1-6. http://doi.org/10.18280/ijei.060101

[23] Von Schuckmann, K., Moreira, L., Cancet, M., Gues, F., Autret, E., Baker, J., Bricaud, C., Bourdalle-Badie, R., Castrillo, L., Cheng, L. (2024). The state of the global ocean. State of the Planet, 4: 1-30. http://doi.org/10.5194/sp-4-osr8-1-2024

[24] Bandyopadhyay, A., Manna, S., Maji, D. (2021). Hydrodynamic aspects of tsunami wave motion: A review. Ocean Dynamics, 71(5): 613-629. http://doi.org/10.1007/s10236-021-01454-z

[25] Firoozi, A.A., Firoozi, A.A. (2024). Non-seismic and

complex source tsunami: Unseen hazard. In Earthquake Ground Motion, IntechOpen. https://doi.org/10.5772/intechopen.1002308
[26] Rossi, G.B., Cannata, A., Iengo, A., Migliaccio, M., Nardone, G., Piscopo, V., Zambianchi, E. (2021). Measurement of sea waves. Sensors, 22(1): 78. https://doi.org/10.3390/s22010078
[27] The Grace of God Almighty Minister of Public Works and Public Housing the Republic of Indonesia. (2016). Regulation of the Minister of Public Works and Public Housing Concerning Unit Price Analysis for Public Works Projects, pp. 1-889.
[28] Abney, S.E., Bright, K.R., McKinney, J., Ijaz, M.K., Gerba, C.P. (2021). Toilet hygiene—review and research needs. Journal of Applied Microbiology, 131(6): 2705-2714. https://doi.org/10.1111/jam.15121
[29] Indonesian National Standard. (2002). Indonesian National Standard on Procedures for Planning Public Toilet Buildings, pp. 1-15. https://akses-sni.bsn.go.id/viewsni/baca/10356.
[30] Fatimah, E., Fauzi, M., Fauzia, A., Kiswanto, K., Abdullah, A., Clara, B.F., Syahna, D. (2023). Determination of design criteria for floating portable toilet applied at flood prone area. International Journal of Disaster Management, 6(2): 251-262. https://doi.org/10.24815/ijdm.v6i2.33651
[31] Munir, V.N, Fauzi, M., Fatimah, A. (2024). Numerical simulation of the stability of floating portable toilet against the influence of waves using DualSPH. Aceh International Symposium on Civil Engineering.
[32] Diyatura, S. (2024). Designing floating portable toilets for flood-prone areas. Universitas Syiah Kuala.
[33] Pozorski, J., Olejnik, M. (2024). Smoothed particle hydrodynamics modelling of multiphase flows: An overview. Acta Mechanica, 235: 1685-1714. https://doi.org/10.1007/s00707-023-03763-4
[34] Long, S., Wong, K. K.L., Fan, X., Gui, X., Yang, C. (2023). Smoothed particle hydrodynamics method for free surface flow based on MPI parallel computing. Frontiers in Physics, 11: 1-17. https://doi.org/10.3389/fphy.2023.1141972
[35] Tan, Z., Sun, P.N., Liu, N.N., Li, Z., Lyu, H.G., Zhu, R.H. (2023). SPH simulation and experimental validation of the dynamic response of floating offshore wind turbines in waves. Renewable Energy, 205: 393–409. https://doi.org/10.1016/j.renene.2023.01.081
[36] Li, Q., Bai, S., Dong, S., Zhou, J., Kitazawa, D. (2024). Experimental and numerical investigation on the motion responses of a spar-type floating structure with aquaculture feeding systems. Journal of Marine Science and Engineering, 12(8): 1329. https://doi.org/10.3390/jmse12081329
[37] Xu, X. (2020). Dynamic analysis of a spar-type offshore floating wind turbine and its mooring system. PhD Thesis, University of Strathclyde.
[38] Pimenta, F., Ruzzo, C., Failla, G., Arena, F., Alves, M., Magalhães, F. (2020). Dynamic response characterization of floating structures based on numerical simulations. Energies, 13(21): 5670. https://doi.org/10.3390/en13215670
[39] Altomare, C., Li, Y.P., Tafuni, A. (2025). Exploring dissipation terms in the SPH momentum equation for wave breaking on a vertical pile. Journal of Marine Science and Engineering, 13(6): 1005. https://doi.org/10.3390/jmse13061005
[40] Ji, C., Hao, Y., Xu, S. (2025). Experimental and numerical study on the hydrodynamic responses of a novel offshore floating photovoltaic system. Ocean Engineering, 315: 119797. https://doi.org/10.1016/j.oceaneng.2024.119797
[41] Jiang, C., Zhang, Q., el Moctar, O., Xu, P., Iseki, T., Zhang, G. (2024). Data-driven modelling of wave–structure interaction for a moored floating structure. Ocean Engineering, 300: 117522. https://doi.org/10.1016/j.oceaneng.2024.117522
[42] Quality System Group of 29th ITTC. (2021). Recommended Procedures and Guideline for Uncertainty Analysis of Resistance Tests in Towing Tanks (Patent 7.5-02-02.02.1).
[43] Liu, K., Chen, D., Liang, P., Yao, X., Deng, Z., Xu, K., Xin, Y., Huang, D. (2025). SPH modeling and experimental validation on power performance and dynamic response of a novel swing-wing wave energy converter. Energy Conversion and Management, 325: 119420. https://doi.org/10.1016/j.enconman.2024.119420
[44] Rizal, N., Sari, D.P. Cahyono, B. Prastyo, D.D., Ali, B., Arianti, E. (2014). Experimental seakeeping and uncertainty analysis of benchmark ship model in regular head and beam waves. Nase More, 70(1): 48-57. https://doi.org/10.17818/NM/2023/1.5